

Simulation Pattern of Forest Cover Change in Onigambari Reserve, Ibadan, Oyo State, Nigeria using spectral vegetation index and Markov chain Techniques

Anthony Tobore (✉ anthonytobore@gmail.com)

Department of Soil Science and Land Management, College of Plant Science and Crop Production, Federal University of Agriculture Abeokuta, Ogun State, Nigeria. P.M.B. 2240, Abeokuta, Ogun State, Nigeria. <https://orcid.org/0000-0002-3645-2864>

Khadijat Alabi

Department of Crop Production, College of Agriculture, Kwara State University, P. M. B. 1530, Malete, Ilorin, Kwara State, Nigeria.

Ganiyu Oyerinde

Department of Soil Science, Faculty of Agriculture, University of Abuja.

Bolarinwa Senjobi

Department of Soil Science and Land Management, College of Plant Science and Crop Production, Federal University of Agriculture Abeokuta, Ogun State, Nigeria. P.M.B. 2240, Abeokuta, Ogun State, Nigeria.

Research Article

Keywords: Forest cover change, spectral vegetation index, cellular automata, Markov chain

Posted Date: February 26th, 2021

DOI: <https://doi.org/10.21203/rs.3.rs-224904/v1>

License: © ⓘ This work is licensed under a Creative Commons Attribution 4.0 International License.

[Read Full License](#)

Simulation Pattern of Forest Cover Change in Onigambari Reserve, Ibadan, Oyo State, Nigeria
using spectral vegetation index and Markov chain Techniques

*Alabi Khadijat¹, Tobore Anthony², Oyerinde Ganiyu³, Senjobi Bolarinwa²

¹Department of Crop Production, College of Agriculture, Kwara State University, P. M. B. 1530,
Malete, Ilorin, Kwara State, Nigeria.

²Department of Soil Science and Land Management, College of Plant Science and Crop
Production, Federal University of Agriculture Abeokuta, Ogun State, Nigeria. P.M.B. 2240,
Abeokuta, Ogun State, Nigeria.

³Department of Soil Science, Faculty of Agriculture, University of Abuja.

Corresponding author: Tobore Anthony.

Corresponding author Email: anthonytobore@gmail.com.

Abstract

Forest cover change (FCC) varies from region to region and is thus considered as one of the
drivers of climate change. This study identified the pattern of the FCC for the years 2010 and
2020 using spectral vegetation index and Markov chain Techniques. The Markov chain (MC)
techniques were utilized to simulate the forest cover map for the year 2030. The spectral
vegetation index of Landsat 7 Enhanced thematic mapper plus (ETM+) and Landsat 8
Operational land images (OLI) were used to assess the forest cover loss for the year 2010 and
2020. Based on the validation result, the accuracy of the forest cover simulation model is more
than 75 percent (%). The simulation result shows that if the current deforestation and
encroachment continues, the forest cover will continue to be endangered and thus leading to a
decrease in dense forest, plantation, and sparse vegetation by 20.9%, 16.1%, and 20%

respectively. This study will assist planners and decision-makers in ensuring sustainable forest management.

Introduction

Forest cover is one of the most important interactions between human and global environmental systems (bonan, 2008). Tropical forest contributes 5 to 15 percent of anthropogenic carbon emissions to the atmosphere at the global, regional, and local scales (d'Annunzioin et al. 2015). Recent reports indicate that forest cover change (FCC) affects the earth's surface and serves as the second-largest source of atmospheric emission (Achard et al. 2002). In addition, deforestation and degradation processes contribute immensely to forest cover loss (Herold et al., 2011a; UNFCCC, 2014). Nevertheless, ninety percent of FCC in sub-Sahara Africa is altered due to an increase in the human population, expansion of agricultural activities, and consistent change of land use especially in Nigeria (Oyerinde et al. 2015; FAO, 1999; Ebenezer 2015). In Nigeria, forests cover approximately covered 35% of the country's landmass (Nweze, 2002; FAO, 2010). The spectral and time-series data provided by satellite images has opened great opportunities in assessing and monitoring FCC at various scales (Hirschmugl et al. 2017). Recently, the Landsat 7 Enhanced Thematic Mapper Plus (ETM+) images, together with Landsat 8 Operational Land Images (OLI) are becoming the driving force of mapping and monitoring FCC due to its availability and accessibility (Hansen et al. 2014). Monitoring and choosing a suitable spectral vegetation index can help to understand the dynamics of forest cover (Pereira et al. 1999). For instance, FCC has been widely monitored using the Normalized difference vegetation index (NDVI) at higher accuracy (Zhu and Liu, 2015). One of the driving mechanisms of modeling FCC is to analyze the past, present, and simulate possible future changes (Wu et al. 2013). However, remote sensing techniques (RST) with

Geographic information system (GIS) are recognized as an indispensable tool in storing, displaying, and analyzing the past, present, and possible future changes through various methods such as Cellular automata models (Clarke et al., 1997), Statistical analysis (Koomen and Beurden, 2011); Markov chain (Wu, 2006), and Artificial neural network (Subedi, and Thapa, 2013). Integration of the Cellular automata (CA) and Markov chain (MC) model are becoming widely used and acceptable for mapping FCC due to their efficiency and high flexibility (Ansari et al. 2016). Adedeji (2001) implemented the CA-Markov to model changes in forest cover in the Onigambari forest reserve. However, the study was limited in assessing the FCC using a spectral vegetation index. Besides, few studies have been applied to integrate spectral vegetation indices and the Markov chain model in simulating forest cover especially in developing countries such as Nigeria. The approach herein implemented the spectral vegetation indices of Landsat 7 ETM+ and Landsat 8 OLI images with a Markov chain model to simulate forest cover in Onigambari forest reserve, Ibadan, Oyo State, Nigeria. Hence, the specific objectives were to (i) assess the forest cover loss for the years 2010 and 2020 using spectral vegetation index (ii) map and simulate the FCC of the study area from the year 2010 to 2030.

Keywords: Forest cover change; spectral vegetation index; cellular automata; Markov chain.

Description of the study area

The study area is located at Ibadan between the Guinea and derived savanna of Oyo State, Southwest Nigeria. The forest reserve falls between latitude 7°25' and 7°55'N and longitude 3°53' and 3°90' E, zones 31 with slopes ranging between 120 to 150 meters above mean sea level (Figure 1). The reserve area extends from Mamu, Onigambari, etc., and covering about 14,506.4 hectares (Akinnifesi and Akinsanmi, 1995). Out of the existing zones, Mamu and Onigambari were predominantly made up of Gmelina plantations while the other existing area comprises

both *Gmelina Arborea* and *Tectona grandis* with natural rainforest tree species (spp) such as *Terminalia* spp *Triplochiton scleroxylon*, *Irvingia garbonensis*, and *Treculia Africana* spp (Akinnifesi and Akinsanmi, 1995).

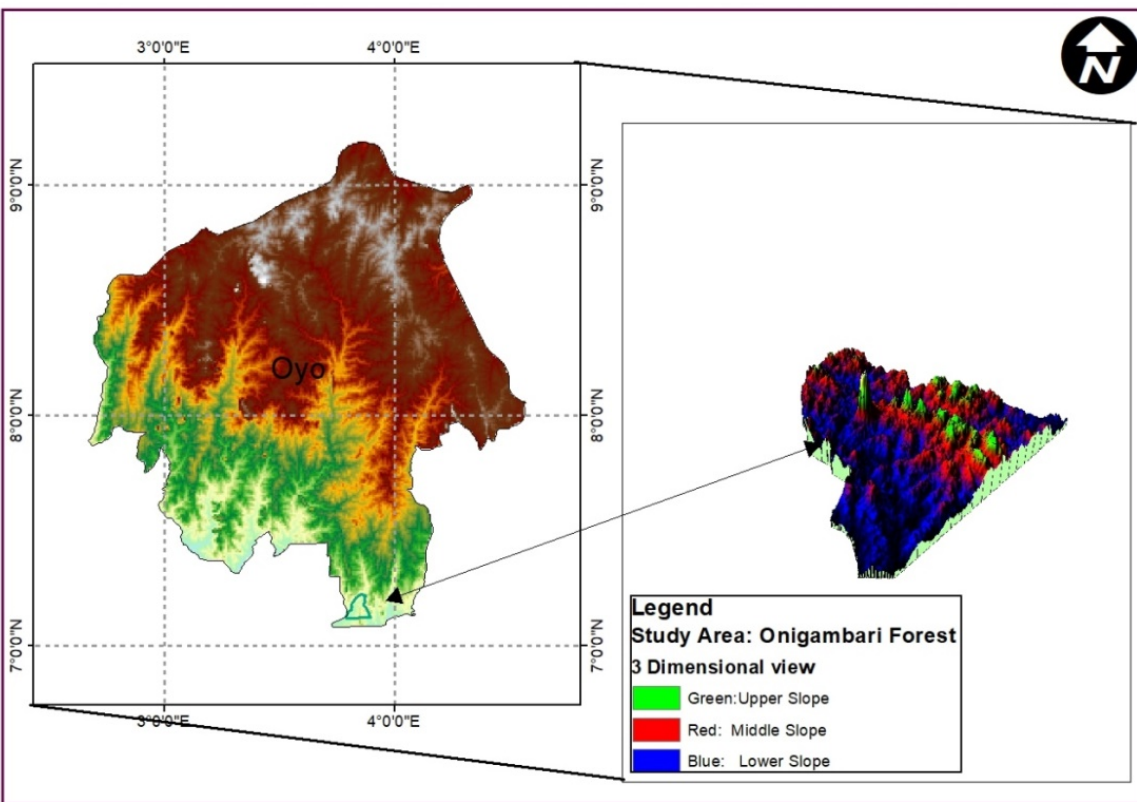


Figure 1: The study area

Climate

The climate of the study area is well-defined dry and wet seasons (Adebekun, 1978). The rainfall starts from May to July with a short dry spell period in August and relative humidity of about 60 to 80 percent which fluctuates during January and February (Larinde and Olasupio, 2011; Oyeniyi and Aweto, 1986). Due to the easy assessment of the study area, the remotely sensed daily climatic data such as average minimum and maximum temperature and rainfall for the study region was obtained and downloaded (<https://power.larc.nasa.gov/>) from the year 2010 to

2019. Thereafter, the rainfall and temperature minimum and maximum data collected (Tmin and Tmax) were then processed according to the mean annual data (figure 2).

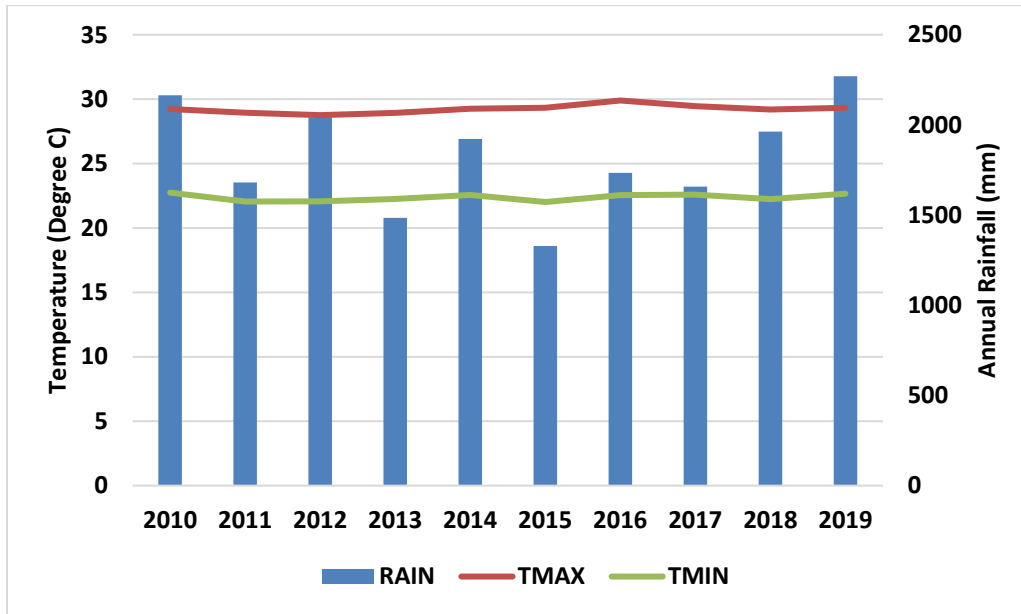


Figure 2: Rainfall and Temperature of the study area

Soil and Geology

The parent material of the study area is derived from the basement complex with intrusions of quartzite, schist, and gneisses (Jones and Wild, 1975). The clay mineral of the area is kaolinite and described as having overlaying low clay activity with a deep soil depth which varies between pedons. The soil particle size distribution classification ranged from sandy clay loam to sandy loam with the presence and formation of the argillic horizon and thus classified as Mollic Cambisols and Abruptic Eutric (FAO/IUSS Working Group, 2010).

Study Methods

Data Sources and description

The fieldwork started with a reconnaissance visit to the study area and was followed by primary data collection. During the reconnaissance survey visit, ground-truthing information was acquired to define the nature of the forest covers with the aid of a GPS (Global positioning

system) device. Written information such as a base map and reports were acquired through downloading from the USGS (United States Geological Survey) repository website. In this study, Landsat 7 ETM+ and Landsat 8 OLI satellite data for the years 2010 and 2020 were acquired and used to assess and simulate the FCC. The downloaded satellite images were geo-rectified according to 31-North UTM (Universal Transverse Mercator) coordinate system using path 191 and row 055 (Table 1). Due to the atmospheric error and avoidance of seasonal variation, the Landsat satellite images were downloaded during the dry season and thus ensure the image is free of noise and no further image-to-image registration. Afterward, the image processing and analyses were executed in ENVI 5.1 software. The result of the image processing and analyses was supported with the images downloaded from the Google Earth Pro engine. The essence of supporting with Google Earth image is to enable easy identification of AOI (Area of interest) during image processing and analyses.

Table 1: Details of the satellite image characteristics

Satellite Image	Acquisition date	Path and row	Used Bands composite	No of bands	Scale/Resolution	Sources
LandSat 7ETM+	06/12/2010	P191, R55	321	8	30m by 30m	USGS
LandSat 8OLI	20/01/2020	P191, R55	432	11	30m by 30m	USGS

Source: USGS

Forest cover assessment using Landsat-8 spectral vegetation index

In the present study, forest cover loss was assessed using Landsat 7 ETM+ and Landsat 8 OLI satellite images of the years 2010 and 2020. The satellite images were subjected to image pre-processing in ENVI environments using DOS (dark object subtraction) method. The DOS method was implemented to improve the visual interpretation and better visibility of Landsat images during analyses. The NDVI (Normalized difference vegetation index), GNDVI (Green

normalized difference vegetation index), and DVI (Difference vegetation index) was used. Thereafter, the spectral vegetation index was assessed and computed in raster math's tool using ArcGIS 10 ESRI (Environmental Software Research Institute). The spectral vegetation index was selected based on their sensitivities and higher accuracy to forest cover monitoring at different scales (Jiang et al. 2006). The selected spectral vegetation index was assessed using the following formula (Table 2).

Table 2: Selected vegetation indices

Spectral Indices	Formula
Normalized Difference Vegetation Index	$NDVI = \frac{(NIR - RED)}{(NIR + RED)}$
Green Normalized Difference Vegetation Index	$GNDVI = \frac{(SWIR2 - GREEN)}{(SWIR2 + GREEN)}$
Difference vegetation index	$DVI = (NIR - RED)$

Sources: (Rouse et al. 1973; Miura et al. 2000; Jiang et al. 2006)

Image Analyses and Processing

The collected Landsat 7 ETM+ and Landsat 8 OLI satellite images were enhanced in ENVI 5.1 Software via (3 by 3) majority filter techniques for better visibility. Natural color composite (NCC) was generated using suitable combinations of bands from the acquired Landsat satellite images (d'Entremont and Thomason, 1987; Good and Giordano, 2019). Considering the "Nigeria Land Classification System" and the goal of this study, Anderson (1976) classification scheme II and reconnaissance survey was utilized to identify the AOI features of the study area. Thereafter, the acquired Landsat images for the years 2010 and 2020 were classified by a supervised classification method in ENVI 5.1 environment. The images obtained from the classified Landsat 7 ETM+ and Landsat 8 OLI was used to identify the forest cover classes based on the Maximum Likelihood Supervised Classification (MLSC) algorithm. The MLSC is applied due to its detail efficiency and easy classification algorithm (Liu 2005; Sun et al. 2013; Biro et al. 2013). The

identified forest cover classes are plantation, agricultural land, dense forest, sparse vegetation, and Bareground (Table 3). The classified images were further imported to iDrasi selva using the Envi-iDrasi format tool. Afterward, the classified forest cover map of the study area was subjected to accuracy and validation using the Kappa coefficient through 100 ground truths field data. These 100 ground truth field data were chosen through the random sampling process. However, for acceptability of the classification accuracy, the classified forest cover classes are over 75% (Pontius Jr and Millones, 2011; Foody, 2002; Story and Congalton, 1986). The Kappa coefficient (K) for the forest cover classification accuracy assessment was shown in Equation (1):

$$K = \frac{\sum_{i=1}^r x_{ii} - \sum_{i=1}^r (x_i \times x + i)}{N^2 - \sum_{i=1}^r (x_i \times x + i)} \dots \dots \dots \text{Equation (1)}$$

The K is the kappa coefficient, N is the total number of sites in the matrix, r is the number of rows in the matrix, x_{ii} is the number in rows i and column i.

Table 3: Definition of Forest cover

No	Land cover classes	Description
1	Plantation	Timber plantations with <i>Tectona arborea</i> and <i>Gmelina</i>
2	Agricultural Land	Arable land, permanent crops, pastures and heterogeneous agricultural areas
3	Dense Forest	Indigenous species such as <i>Terminalia</i> spp, <i>Triplochiton scleroxylon</i> , <i>Irvingia garbonensis</i> , and <i>Treculia Africana</i>
4	Sparse vegetation	Secondary forest, Shrubs and/or herbaceous vegetation association,
5	Bareground	Permanently degraded land, bare ground, rock, quarry despoiled lands

Simulation Pattern Analysis

To simulate the FCC of the study area, the Markov-chain model was used to determine the forest cover pattern for the year 2030. The Cellular automata were used to stimulate the time-space and underlie the dynamics of changes in the study area (Balogun and Ishola, 2017). However, the

Markov chain and cellular automata were further supported with dependent and independent variables in the iDrise selva environment. The independent variables are the classified forest cover maps of the year 2010 and 2020 of the present study. For the dependent variable, open shape-files data and SRTM (Shuttle radar topographic mapper) image of 30 meters resolution was downloaded and acquired from the USGS website. The dependent variable used in this study includes; Digital elevation model (DEM), aspect, distance from major/minor road, and distance from the river (Figures 3a and 3b). The downloaded SRTM image and open shape-file data of the study area were clipped in ArcGIS 10 ESRI. The clipped SRTM was used to produce the DEM and aspect map of the study area using a raster surface processing tool. The Euclidean distance tool operation was used to produce the distance from the river and the major road of the study area. Thereafter, the independent and dependent variables were used as input parameters to generate the transition probability matrix from the Markov-chain and further used as inputs for the Cellular automata in the iDrise selva environment. Based on the transition probability matrix between the year 2010 and 2020 classified images, the forest cover map for the year 2030 was predicted. The Cellular automata and Markov chain model used in this study were described according to Subedi et al. (2013) in equations (2) and (3). The conceptual framework of the present study was shown in figure (4).

$$S_t^{+1} = f(S_t, N) \dots \dots \dots \text{Equation 2}$$

Here, S represents the set of states of the finite cells; t and t+1 are the early years and the later year; N is the neighborhood of cells, and f is the conversion rule of local space.

$$\begin{bmatrix} P_{11} & P_{12} & \dots & P_{1n} \\ \vdots & & \ddots & \vdots \\ P_{n1} & P_{n2} & \dots & P_{nn} \end{bmatrix} \dots \dots \dots \text{Equation 3}$$

Where P stands for the probability matrix in the Markov model, and P_{ij} is the probability of converting from current state i to state j in the next period. S is the land use status, and t ; $t + 1$ is the time point and this was described according to Subedi et al. (2013) using Equation (4).

$$0 < P_{ij} < 1 \text{ and } \sum_{j=1}^n P_{ij} = 1, i, j = 1, 2, 3 \dots n. \dots \dots \dots \text{Equation 4}$$

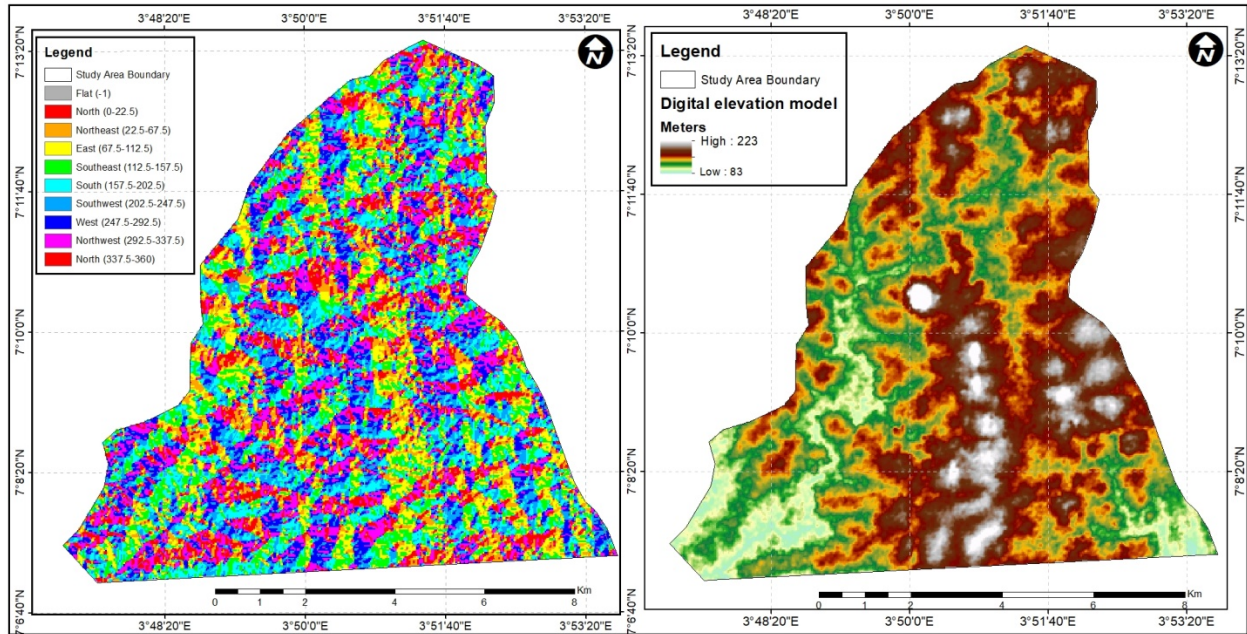


Figure 3a: Aspect and Digital elevation model of the study area.

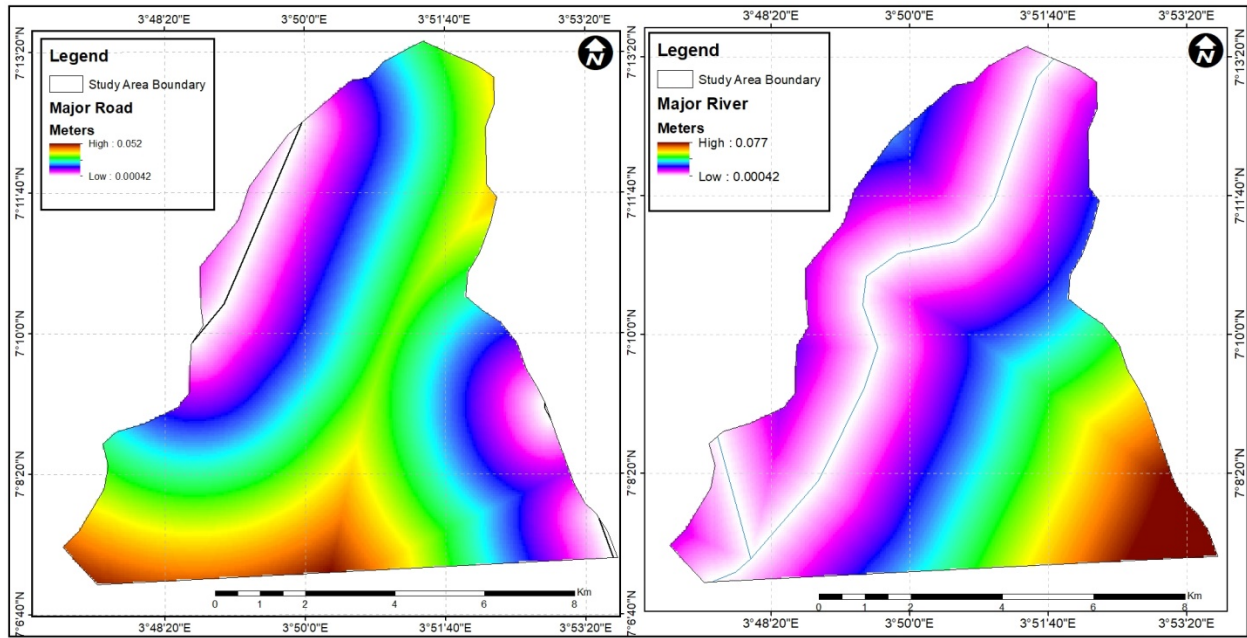


Figure 3b: Major Road and River of the study area.

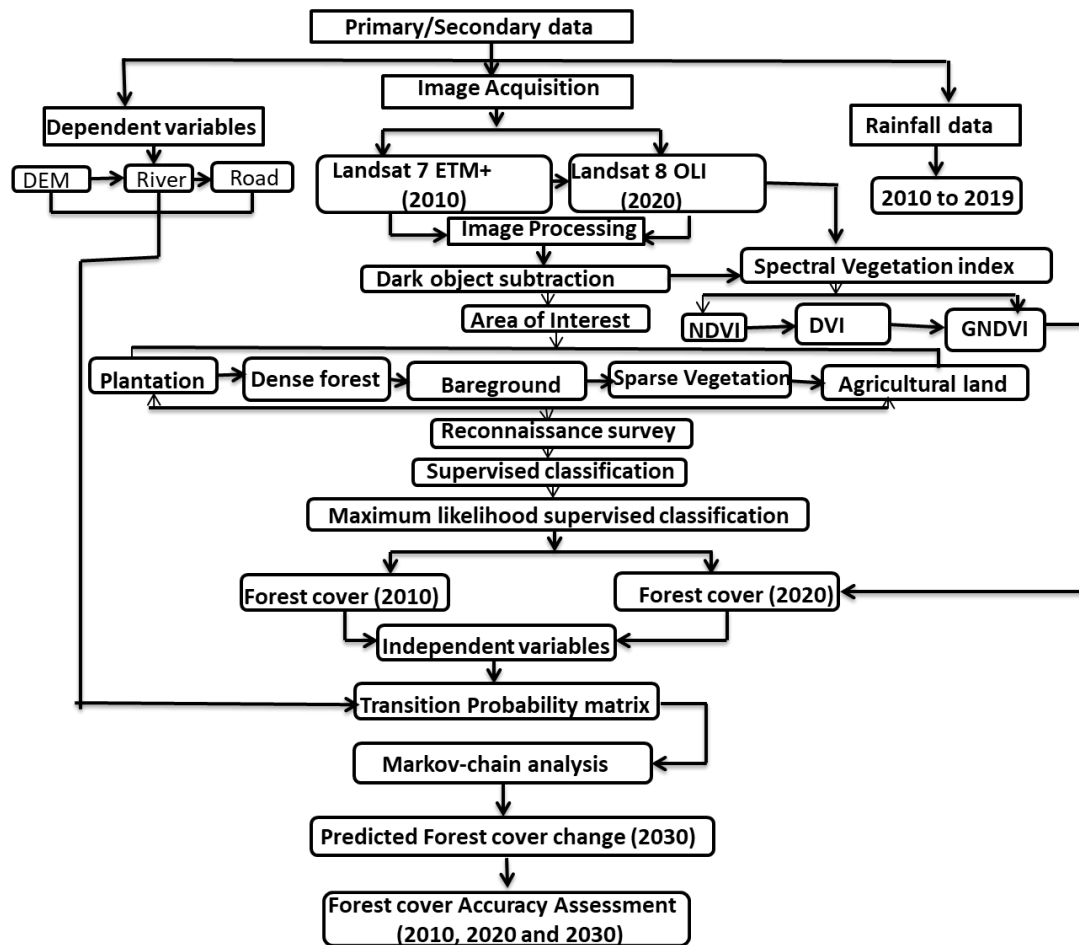


Figure 4: Conceptual framework of the study area.

Results and Discussion

The sensitivity of spectral vegetation indices

The present study utilized the Landsat 7 ETM+ and Landsat 8 OLI spectral vegetation index of the year 2010 and 2020 to assess the rate of forest cover loss. The NDVI, GNDVI, and DVI of the study area were classified as (-1) low and (1) high. The result of the NDVI, GNDVI, and DVI reveals that the study area demonstrates low forest cover densities in the year 2020 than the year 2010 (Figures 5, 6, and 7). However, it was also observed during the reconnaissance survey that the forest cover of the present study had experienced consistent changes such as an expansion of agricultural practices, and degradation of the study area. Besides, the sensitivity of the spectral vegetation index used in this study has also provided evidence and easy assessment of the past and present forest cover of the study area. According to Aman et al. (1992), the abrupt or gradual change of the past, present and possible future changes of forest cover are better assessed using spectral vegetation index. Warner et al. (2016) also highlighted that mapping and monitoring forest cover changes using NDVI, DVI, and GNDVI are regarded as one of the most correlated spectral vegetation indices with higher validation accuracy. Also, the present study interdem with the study conducted by Oyerinde et al. (2015) that Nigeria forest cover is faced with sudden and gradual deforestation.

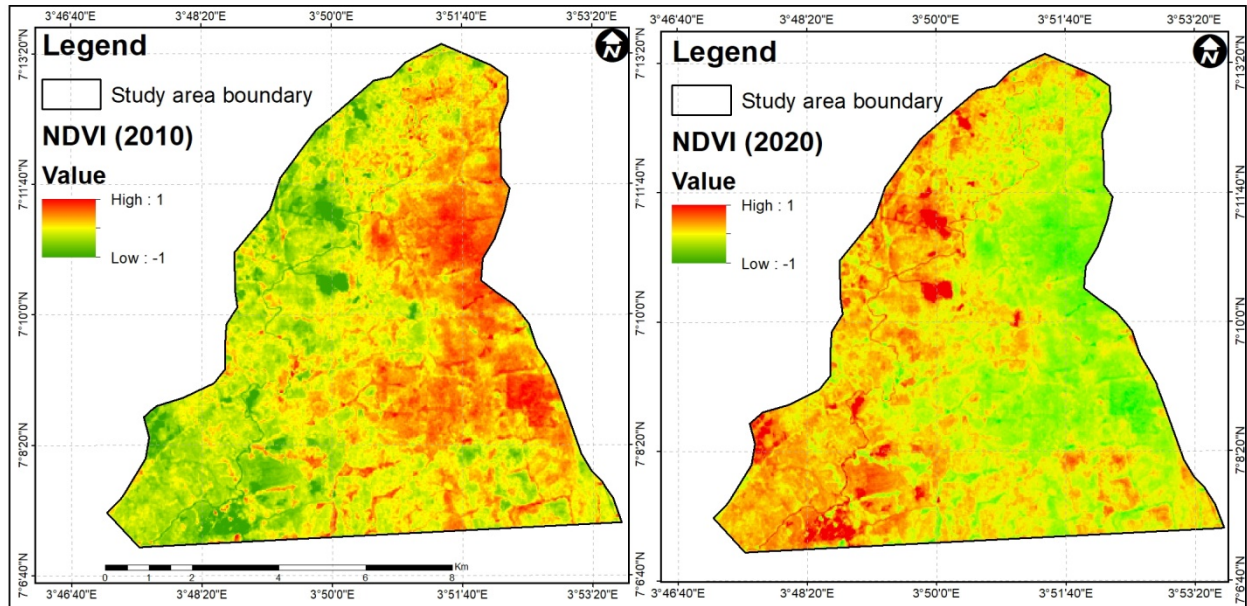


Figure 5: Normalized difference vegetation index of the study area

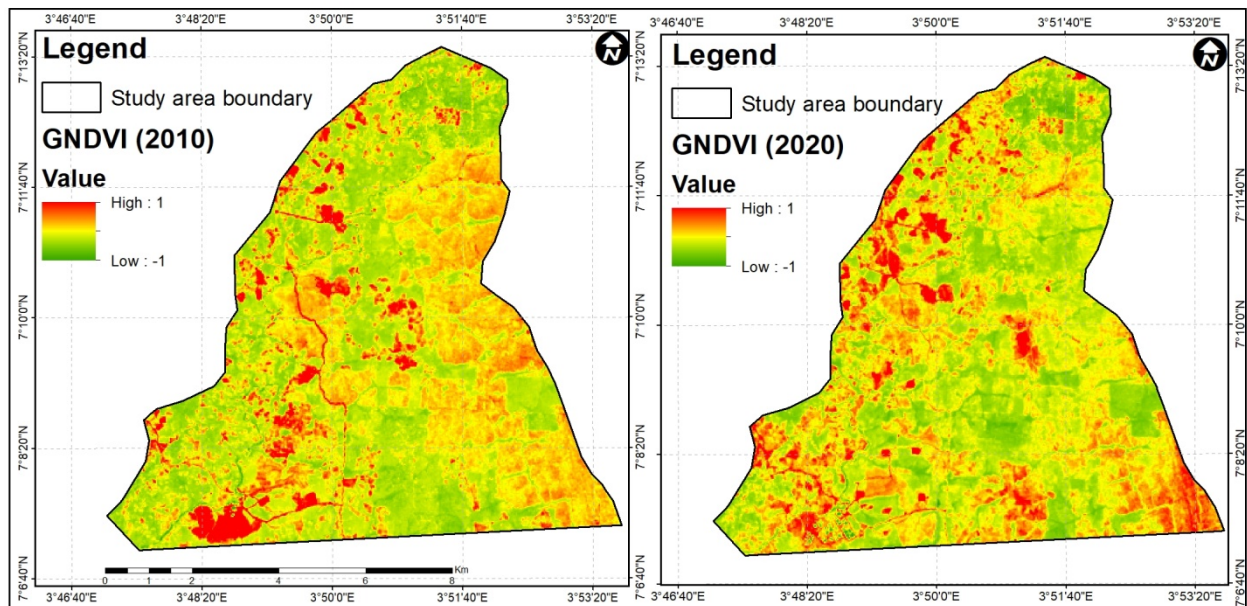


Figure 6: Green Normalized vegetation index of the study area

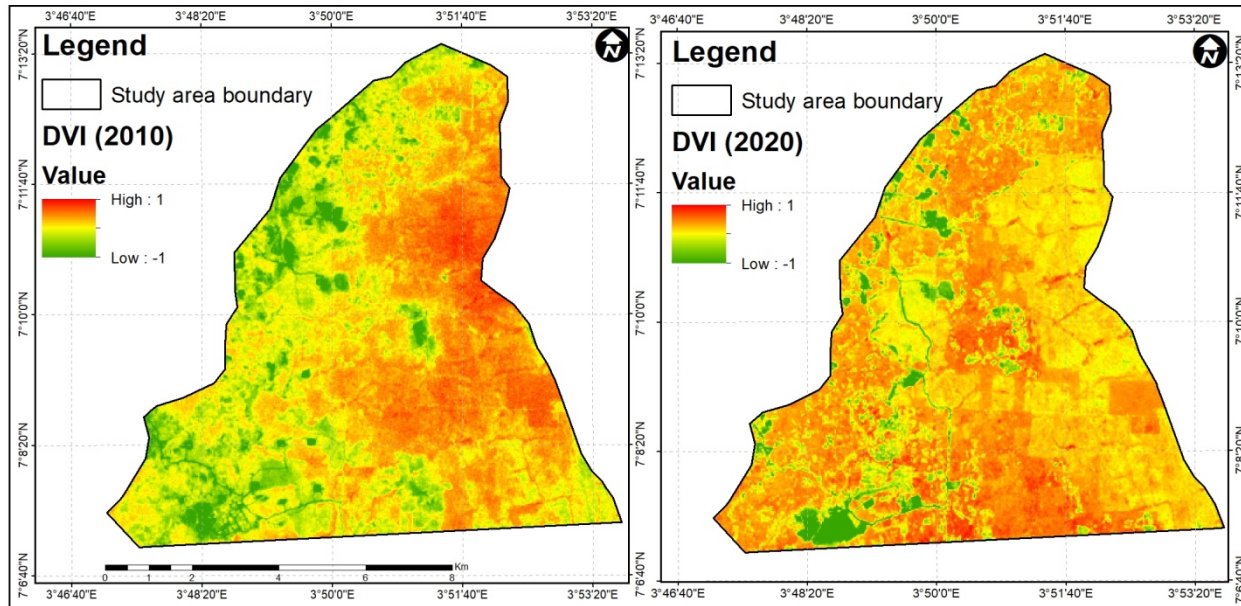


Figure 7: Difference vegetation index of the study area

Forest cover mapping from 2010 to 2030

The periodical assessment characteristics and the analyzed Natural color composite (NCC) were used to specifically classify the forest cover of the study area. In the present study, the MLSC algorithm was applied to the Landsat 7 ETM+ and Landsat 8 OLI satellite images for the year 2010 and 2020 focusing on Plantation (PL), Agricultural land (AL), Dense forest (DF), Sparse vegetation (SV), and Bareground (BG) using the Envi 5.1 software (Figure 8). The CA-Markov model was implemented and subjected to visual image interpretation, cognition of patterns, and colors which shows great efficiency in simulating the year 2030 forest cover map of the study area (Figure 9). Bakx et al. (2019) and Bank (1991) posits that one of the easy and accurate ways of extracting information from remotely sensed data such as Landsat satellite images is by cognition of patterns and colors. The overall classification accuracy for the years 2010, 2020, and 2030 of the forest cover map was 80.00%, 81.47%, and 89.77%. After the prediction, it was found out that the Cohen kappa statistics were > 0.75 and thus shows substantial classification agreement with the present study (Tables 4, 5, and 6). According to Li, (2005) kappa statistics

remains one of the standard procedures of validating the accuracy of classified Landsat images at different levels. The statistical analysis of the multi-temporal forest cover maps revealed that significant changes have taken place in the study area. From the statistical change analysis, it was observed that the AOI features in the year 2010 are in the following order: 34.6% (plantation), 27.4% (sparse vegetation), 24.6% (dense forest), 11.4% (bareground), and 2.0% (agricultural land). However, the significant changes observed from the year 2020 forest cover classification map revealed that plantation, sparse vegetation, and dense forest decreased from 34.6% to 25.9%, 27.4% to 21.0%, and 24.6% to 22.5% while agricultural land and bareground increased from 291.7 Ha (Hectares) to 1000.0 Ha and 1654.1 Ha to 3453.3 Ha (Table 7). However, the increase observed in the agricultural land and bareground translated to the decrease in the dense forest, plantation, and sparse vegetation in the year 2030. Also, the decrease observed in the forest cover features (such as dense forest) in the year 2030 can be attributed to the persistent increase of human activities in the study area. Garg et al. (2006) and Adepoju et al. (2006) noted that a substantial increase in anthropogenic activities such as deforestation and expansion of agricultural practices are known to be one of the major factors contributing to the sudden or gradual loss of forest cover at various scales. Moreover, the rate of deforestation and the substantial loss of forest cover in the study area could also support the gradual or sudden increase of climate change. Abubakar et al. (2014); and Lepers et al. (2005) stated that deforestation is one of the main driving forces predicted to forest cover change in developing countries such as Nigeria. The present study also interdem the view of Akinsoji, (2013) that tropical forests are faced with persistent encroachment of human activities such as deforestation and expansion of agricultural activities.

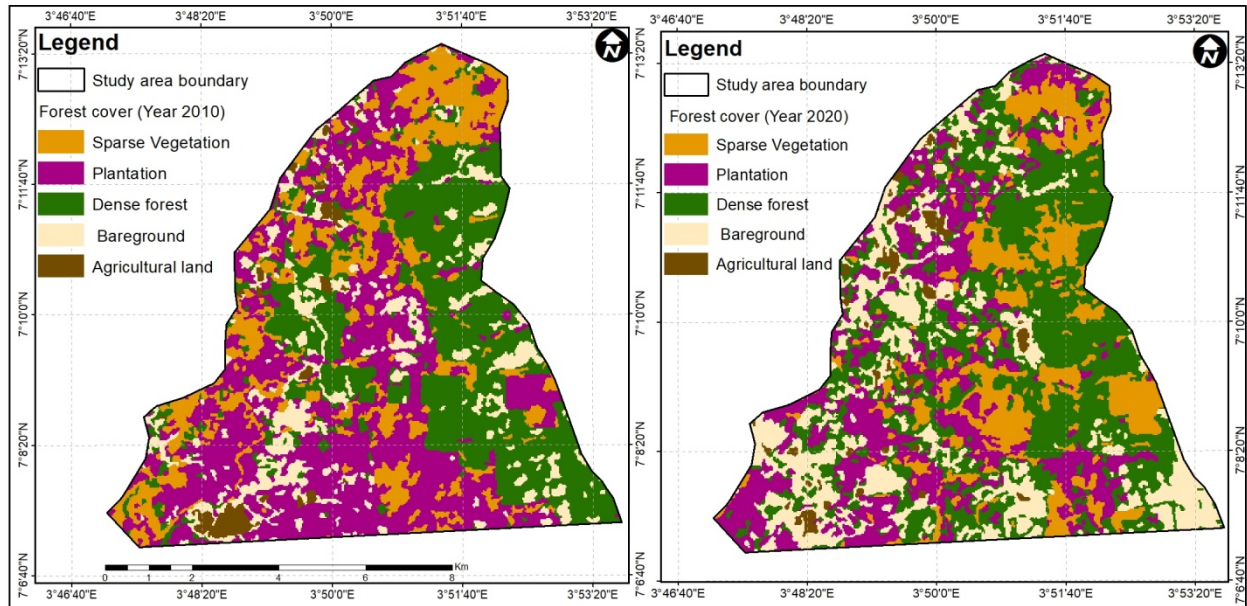


Figure 8: Forest cover map for the year 2010 and 2020

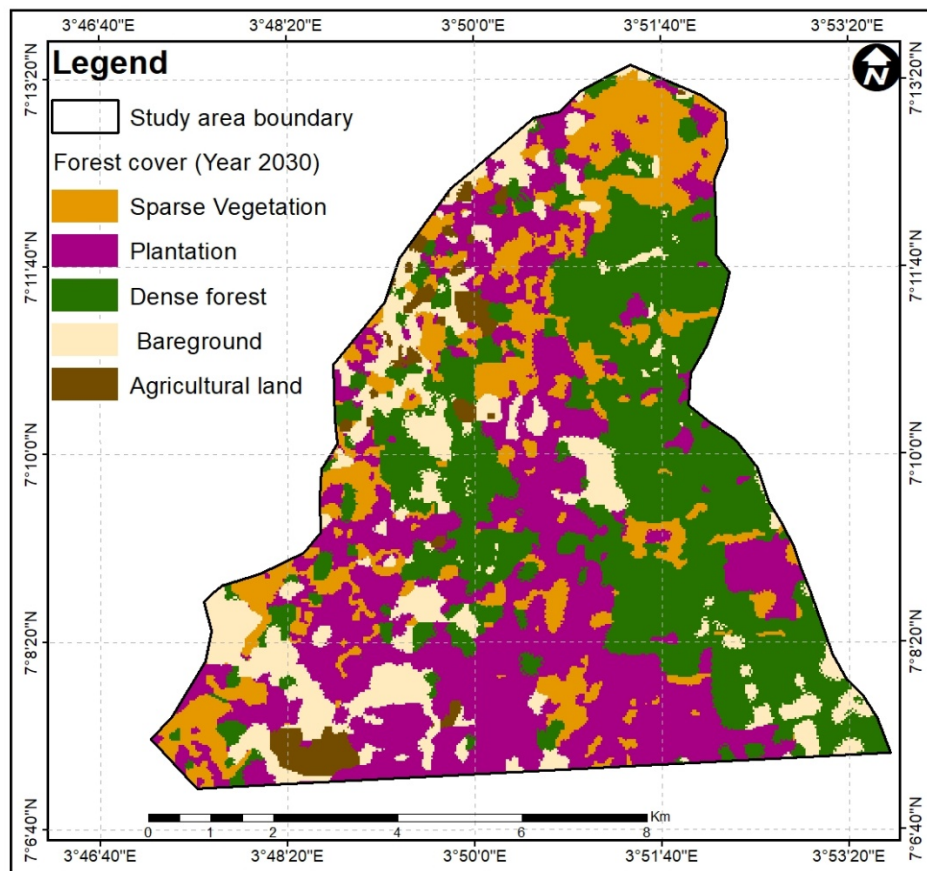


Figure 9: Forest cover map for the year 2030

250 **Table 4: Error Matrix of the study area for the year 2010**

Forest cover	SV	PL	DF	BG	AL	Total	Producer Accuracy (%)	User Accuracy (%)
SV	41	4	0	1	5	51	74.60	80.40
PL	0	54	8	3	0	65	87.10	83.10
DF	4	0	54	0	6	64	65.10	84.40
BG	0	4	3	84	0	91	90.30	92.30
AL	10	0	18	5	43	76	79.60	56.60
Total	55	62	83	93	54	347		
Overall accuracy = 80.00% Kappa coefficient = 75.00%								

251 SV: Sparse vegetation; PL: Plantation; DF: Dense forest; BG: Bareground; AL: Agricultural

252 **Table 5: Error Matrix of the study area for the year 2020**

Forest cover	SV	PL	DF	BG	AL	Total	Producer Accuracy (%)	User Accuracy (%)
SV	51	4	2	1	0	58	78.50	87.93
PL	2	41	4	0	3	50	54.70	82.00
DF	2	10	67	2	0	81	87.01	82.71
BG	10	0	0	80	4	94	85	85.10
AL	0	20	4	0	60	84	71.42	71.4
Total	65	75	77	83	67	367		
Overall accuracy = 81.47% Kappa coefficient = 76.25%								

253 SV: Sparse vegetation; PL: Plantation; DF: Dense forest; BG: Bareground; AL: Agricultural

254 **Table 6: Error Matrix of the study area for the year 2030**

Forest cover	SV	PL	DF	BG	AL	Total	Producer Accuracy (%)	User Accuracy (%)
SV	30	1	2	1	1	35	69.76	85.71
PL	2	51	0	0	0	53	79.68	96.22
DF	1	0	70	2	0	73	92.10	95.89
BG	5	2	4	76	0	87	96.20	87.35
AL	5	10	0	0	89	104	98.88	85.57
Total	43	64	76	79	90	352		
Overall accuracy = 89.77% Kappa coefficient = 85.89%								

255 SV: Sparse vegetation; PL: Plantation; DF: Dense forest; BG: Bareground; AL: Agricultural

256 **Table 7: Forest cover classification of the study area**

LULC	2010	2020	2030
------	------	------	------

	Ha	%	Ha	%	Ha	%
Sparse vegetation	3972.2	27.4	3042.8	21	2901.6	20
Plantation	5026.2	34.6	3752.6	25.9	2338.3	16.1
Dense forest	3562.2	24.6	3257.7	22.5	3034.9	20.9
Bareground	1654.1	11.4	3453.3	23.8	4914.3	33.9
Agricultural Land	291.7	2	1000	6.9	1317.3	9.1
Total	14506.4	100	14506.4	100	14506.4	100

Conclusion

This study intended to evaluate the significance of FCC in Onigambari forest reserve Ibadan, Oyo State, Nigeria using spectral vegetation index and Markov chain model. Prediction of future forest cover changes shows that such kind of prediction can help to manage the gradual or sudden change of forest cover caused by anthropogenic activities such as deforestation and expansion of agricultural practices. The use of spectral vegetation index reveals that NDVI, GNDVI, and DVI serve as indispensable techniques used in assessing and monitoring forest cover loss with higher accuracy and less time. Based on the forest cover analysis, it was discovered that the forest cover pattern varied significantly from the year 2010 to 2030. The findings of the FCC reveals that the dense forest, plantation, and sparse vegetation will decrease by 20.9%, 16.1%, and 20%, while bareground and agricultural land will increase by 33.9%, and 9.1% respectively. This indicates that the Onigambari forest reserve experienced deforestation and expansion of agricultural activities thereby contributing to climate change. The present study demonstrated the efficiency of GIS and RST in the study of FCC using the spectral vegetation index and Markov chain model.

Acknowledgment

The authors are sincerely grateful to the authority of the Onigambari forest reserve for their understanding and for allowing us to carry out this study. We are equally thankful to the United States Geological Survey (USGS) for assisting this research with data-sets.

Funding

This research did not receive any specific grant from funding agencies in the public, commercial, or not-for-profit sectors.

Declarations of interest

None.

References

- Abubakar, A., Abdulkadir, A. Jibrin, A. and Abubakar, R. B., 2014. An Appraisal of Forest Degradation and Carbon Sequestration of Effan Forest Reserve in Kwara State. *Global Journal of Science Frontier Research: Environment and Earth Sciences*, 14(3), 57-65.
- Achard, F., Eva, H.D., Stibig, H.J., Mayaux, P., Gallego, J., Richards, T., and Malingreau, J.P., 2002. Determination of deforestation rates of the world's humid tropical forests. *Science* 297(5583), 999-1002.
- d'Annunzio R, Sandker M, Finegold Y, Min Z 2015. Projecting global forest area towards 2030. *Forest Ecol Manage* 352(7):124–13
- Adebekun, O., 1978. Atlas of the Federal Republic of Nigeria. 1st Edn., Under the Chairmanship of the National Atlas Committee, pp: 136.
- Adedeji, O.H., 2001. Tropical Forest Dereservation and Degradation: Challenges to Stabilizing Soil Resources and Sustainable Development in Nigeria. Knowledge Review. A Multidisciplinary Journal of National Association for the Advancement of Knowledge, 4, 114-126.
- Anderson, J. R., Hardy, E.E., Roach, J.T., Witmer, R.E., 1976. A land use and land cover classification system for use with remote sensor data: U.S. Geological Survey Professional paper 964.
- Adepoju, M.O., Millington, A.C., Tansey, K.T., 2006. Land Use/Land Cover Change Detection in Metropolitan Lagos (Nigeria):1984–2002, American Society for Photogrammetry and Remote Sensing, Annual Conference, Reno, Nevada, May 1–5.
- Akinnifesi, F.K., Akinsanmi, F.A., 1995. Linear Equations for Estimating the Merchantable Wood Volume of *Gmelina arborea* in Southwest Nigeria. *Journal of Tropical Forest Science*, 7, 391-397.
- Akinsoji, A., 2013. Vegetation Analysis of NgelNyaki Forest Reserve, Mambilla Plateau Nigeria. *Journal of Natural Science Research*, 3(12), 121-125.

308 Ansari, A., 2016. The final report of the research project “Identification of harvesting centres’
 309 and effective factors of dust storms in Mighan Desert Wetland” Arak University.

310 Bakx, T. R. M., Koma, Z., Seijmonsbergen, A. C., Kissling, W. D., 2019. Use and categorization
 311 of LiDAR vegetation metrics in avian diversity and species distribution research. Dryad Digital
 312 Repository. <https://doi.org/10.5061/dryad.tm28hb6>.

313 Balogun, I., Ishola, K., 2017. Projection of future changes in landuse/landcover using cellular
 314 automata/markov model over Akure city, Nigeria. *Journal of Remote Sensing Technology*. 5 (1),
 315 534 22–31.

316 Biro, K., Pradhan, B., Buchroithner, M., and Makeschin, F., 2013. Land use/Land cover change
 317 analysis and its impact on soil properties in the northern part of Gadarifregion, Sudan, Land
 318 Degrad.Dev., 24, 90–102. <https://doi.org/10.1002/ldr.1116>, 2013.

319 Bonan G., 2008. Forest and climate change: forcing, feedbacks and the climate benefits of
 320 forests. *Science* 320(5882):1444–1449.

321 Clarke, K.C., Hoppen, S., Gaydos L. 1997. A self-modelling cellular automata model of
 322 historical urbanization in the San Francisco bay area. *Environ. Plan*, 24: 247-261.

323 d’Entremont, R.P., Thomason, L.W., 1987. Interpreting meteorological satellite images using a
 324 color-composite technique. *Bull. Am. Meteorol. Soc.* 68 (7), 762–768.

325 Ebenezer, T., 2015. Drought, Desertification and The Nigerian Environment : A Review 7, 196–
 326 209. <https://doi.org/10.5897/JENE2015>.

327 FAO., 2010. Global Forest Resources Assessment 2010 – Main report.FAO Forestry Paper No.
 328 163, Rome. Online available at: www.fao.org/docrep/013/i1757e/i1757e00.htm.

329 FAO/IUSS Working Group., 2010. A framework for land evaluation. Rome: Soils Bulletin 31,
 330 FAO, pp 25-42.

331 FAO., 3rd Edition., 1999. State of the World’s Forests. Food and Agriculture Organization of
 332 the United Nations, Rome. <http://www.fao.org/forestry/FO/SOFO/SOFO99/sofo99-e.stm> or
 333 <http://www.fao.org/forestry/en/>

334 Fasola, T.R., 2007. Controlling the Advancement of Savanna into Southwestern Nigeria.
 335 *Zonas Áridas*, 11, 251-259.

336 Foody, G.M., 2002. Status of land cover classification accuracy assessment. *Remote Sens.*
 337 *Environ.* 80 (1), 185–201.

338 Garg, S. K., Garg, R. and Garg, R., 2006. Environmental Science and Ecological Studies,
 339 Khanna Publishers, New Delhi, India.

340 Good, T., Giordano, P.A., 2019. Methods for Constructing a Color Composite Image: Google
341 Patents.

342 Hansen, M. C., Potapov, P. V., Moore, R., Hancher, M., Turubanova, S.A., Tyukavina, A.,
343 Thau, D., Stehman, S. V., Goetz, S. J., Loveland, T. R., Kommareddy, A., Egorov, A., Chini, L.,
344 Justice, O.L., Townshend, J. R. G., 2014. High-Resolution Global Maps of 21st-Century Forest
345 Cover Change. *Science*, 850–53.

346 Herold, M., Hirata, Y., Van Laake, P., Asner, G., Heymell, V., Román-cuesta, R.M., 2011a. A
347 review of methods to measure and monitor historical forest degradation. *Victoria*, 62, 1–31.

348 Hirschmugl, M., Gallaun, H., Dees, M., Datta, P., Deutscher, J., Koutsias, N., Schardt, M., 2017.
349 Methods for Mapping Forest Disturbance and Degradation from Optical Earth Observation Data:
350 a Review. *Current Forestry Reports*, 3, 32–45.

351 Jones, M.J. and Wild, A., 1975. Soils of the West African Savanna, the Maintenance and
352 Improvement of Their Fertility. Commonwealth. Agricultural Bureau, 246.

353 Jiang, Z.; Huete, A.R.; Chen, J.; Chen, Y.; Li, J.; Yan, G.; Zhang, X. 2006. Analysis of NDVI
354 and scaled difference vegetation index retrievals of vegetation fraction. *Remote Sens. Environ.*,
355 101, 366–378.

356 Larinde, S.L. and Olasupo, O.O., 2011. Socio-Economic Importance of Fuelwood Production in
357 Gambari Forest Reserve Area, Oyo State, Nigeria. *Journal of Agriculture and Social Research*
358 (JASR), 11.

359 Lepers, E., Lambin, E F., Janetos, A C., DeFries, R., Achard, F., Ramankutty, N., Scholes, R J.,
360 2005. A synthesis of information on rapid land-cover change for the period 1981–2000.
361 *Bioscience*, 55, 115–24. doi:10.1641/0006-3568(2005)055[0115:ASOIOR]2.0.CO;2.

362 Liu, H., 2005. Accuracy analysis of remote sensing change detection by rule-based rationality
363 evaluation with post-classification comparison. *International Journal of Remote Sensing*, 25(5),
364 1037–1050. <http://dx.doi.org/10.1080/0143116031000150004>

365 Miura, T.; Huete, A.; Yoshioka, H. 2000. Evaluation of sensor calibration uncertainties on
366 vegetation indices for MODIS. *IEEE Trans. Geosci. Remote Sens.* 38, 1399–1409.

367 Nweze, N. J., 2002. Implementing Effective Local Management of Forest Resources in Poor
368 Forest Community of Nigeria. In: Onokala P. C, Phil-Eze P.O, Madu. I. A (eds) *Environment*
369 *and Poverty in Nigeria*, Enugu Jamoe Pub.

370 Oyeniyi, O.L. and Aweto, A.O., 1986. Effects of Teak Planting on Alfisols Topsoil in
371 Southwestern Nigeria. *Singapore Journal of Tropical Geography*, 7, 145–151.
372 <http://dx.doi.org/10.1111/j.1467-9493.1986.tb00178.x>

373 Oyerinde, G.T., Hountondji, F.C.C., Wisser, D., Diekkruger, B., Lawin, A.E., Odofin, A.J.,
374 Afounda, A., 2015. Hydro-climatic changes in the Niger basin and consistency of local
375 perceptions. *Reg. Environ. Chang.* 15, 1627–1637. Doi:10.1007/s10113-014-0716-7.

376 Pereira, J.M.C.; Pereira, B.S.; Barbosa, P.; Stroppiana, D.; Vasconcelos, M.J.P.; Grégoire, J.-M.,
377 1999. Satellite monitoring of fire in the EXPRESSO study area during the dry season
378 experiment: Active fires, burnt area, and atmospheric emissions. *J. Geophys. Res. Atmos.*, 104,
379 30701–30712.

380 Pontius Jr., R.G., Millones, M., 2011. Death to Kappa: birth of quantity disagreement and
381 allocation disagreement for accuracy assessment. *International Journal of Remote Sensing*, 32
382 (15), 4407–4429.

383 Rouse, J.W.; Haas, R.H.; Schell, J.A.; Deering, D.W. 1973. Monitoring vegetation systems in the
384 Great Plains with ERTS. In *Proceedings of the 3rd ERTS Symposium*, Washington, DC, USA,
385 10–14 December; NASA-SP-351-Vol-1-Sect-A. Volume 1, pp. 309–317.

386 Story, M., Congalton, R.G., 1986. Accuracy assessment: a user's perspective. *Photogramm. Eng.*
387 *Rem. Sens.* 52 (3), 397–399.

388 Subedi, P., Thapa, B., 2013. Application of a Hybrid Cellular Automaton–Markov (CA-Markov)
389 Model in land use change prediction: A case study of Saddle Creek Drainage Basin, Florida. *Apl.*
390 *Ecol. Environ. S.* 1(6), 126–132.

391 Subedi, P., Subedi, K., Thapa, B. 2013. Application of a hybrid cellular automaton Markov (CA-
392 Markov) Model in land-use change prediction: a case study of saddle creek drainage Basin,
393 Florida. – *Applied Ecology and Environmental Sciences* 1(6): 126–132.

394 Sun, Y., Zhou, Q., Xie, X., & Liu, R., 2013. Spatial, sources and risk assessment of heavy metal
395 contamination of urban soils in typical regions of Shenyang, China. *Journal of Hazardous*
396 *Materials.* 174(1–3), 455–462. <https://doi.org/10.1016/j.jhazmat.2009.09.074>.
397

398 UNFCCC, 2014. Key Decisions Relevant for Reducing Emissions From Deforestation and
399 Forest Degradation in Developing Countries (REDD+). *Framew. Conv. Clim. Chang.* pp. 44.

400 United Nations., 2010. *World Urbanization Prospects: The Revision United Nations (Population*
401 *Division of the Department of Economic and Social Affairs)* New York. ESA/P/WP/224, 2012.

402 USGS Landsat Missions. Available online: [https://www.usgs.gov/land](https://www.usgs.gov/land-resources/nli/landsat/landsat-data_access)
403 [resources/nli/landsat/landsat-data_access](https://www.usgs.gov/land-resources/nli/landsat/landsat-data_access) (access year 2010 and 2020).

404 Bank, 1991. *Forest Sector Policy Paper*. The World Bank. Washington. DC

- 405 Wu C.D., Cheng C.C., Lo H.C., Chen Y.K., 2013. Application of SEBAL and Markov Models
406 for Future Stream Flow Simulation Through Remote Sensing. *Water Resource Management*.
407 24(14):3773–97. <https://doi.org/10.1007/s11269-010-9633-9>.
- 408 Wu, F., 1998. Simland: a prototype to simulate land conversion through the integrated GIS and
409 CA with AHP-derived transition rules. *International Journal of Geographical Information*
410 *Science*. 12, pp. 63-82.
- 411 Zhu, X.; Liu, D., 2015. Improving forest aboveground biomass estimation using seasonal
412 Landsat NDVI time-series. *ISPRS Journal of Photogrammetry Remote Sensing*, 102: 222 – 231.

Figures

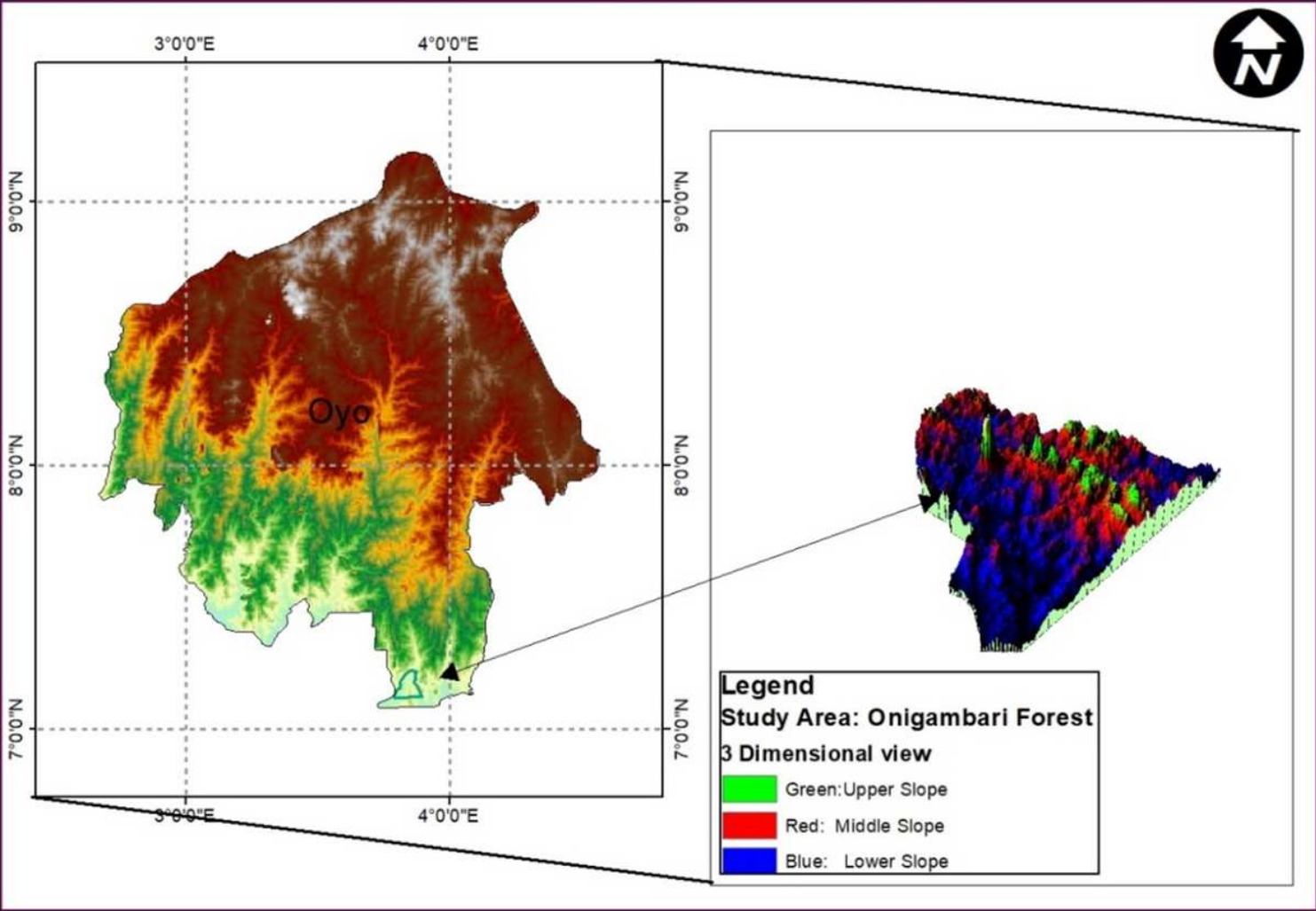


Figure 1

The study area

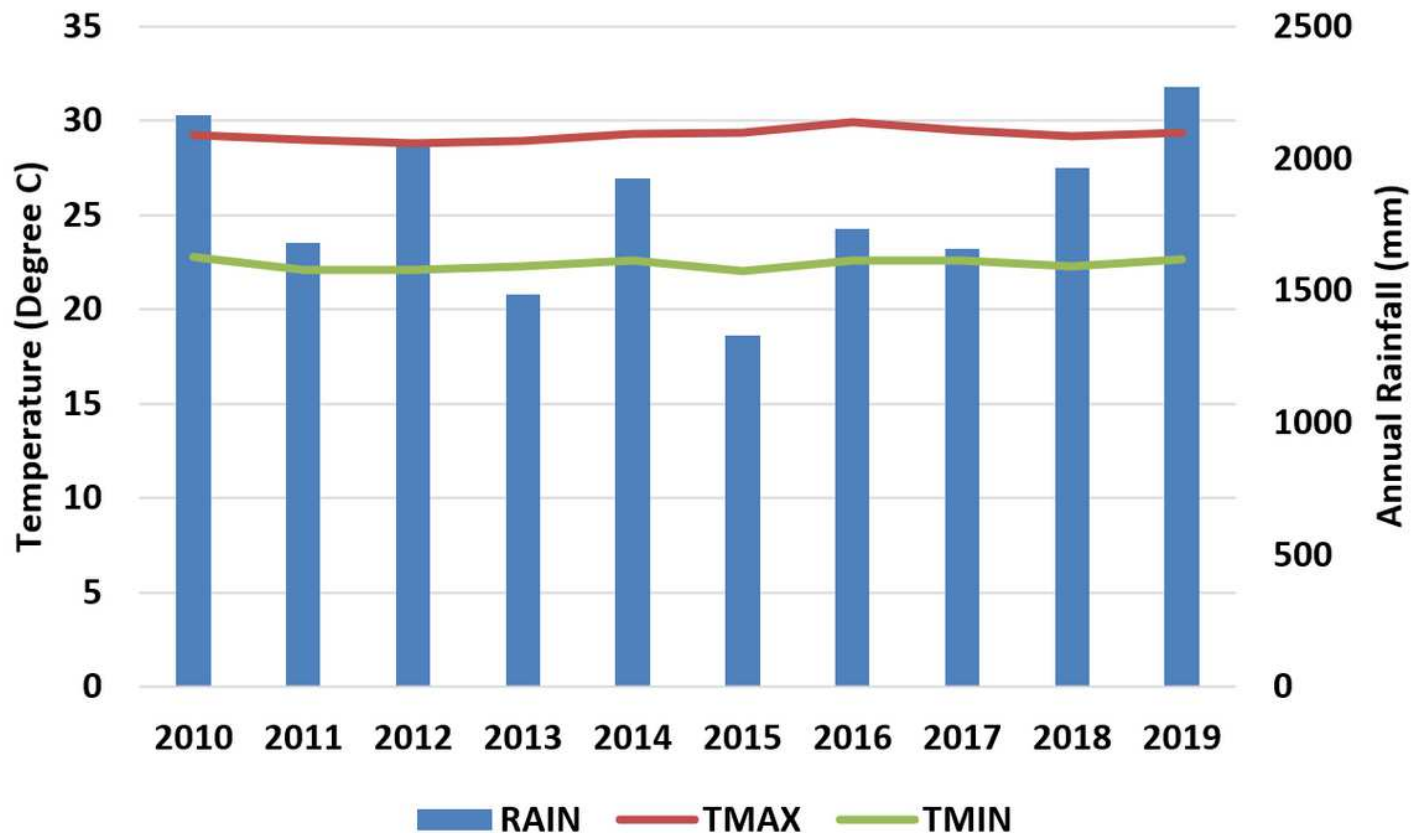


Figure 2

Rainfall and Temperature of the study area

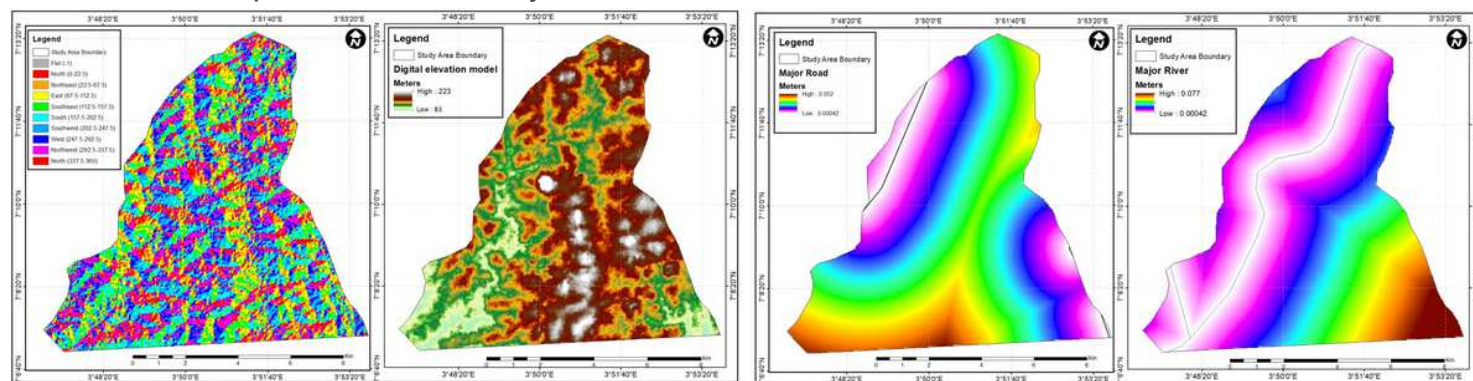


Figure 3

a: Aspect and Digital elevation model of the study area. b: Major Road and River of the study area.

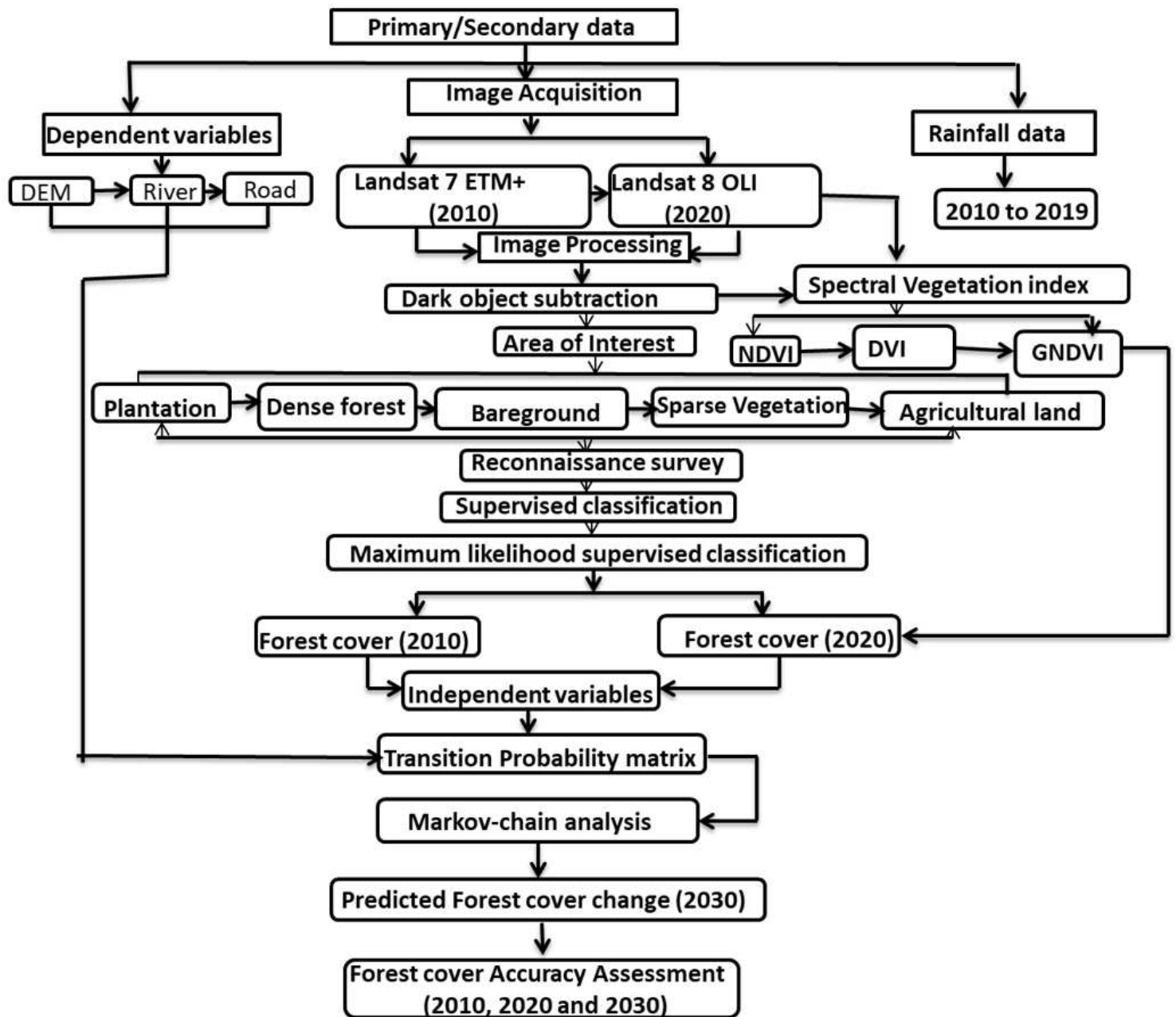


Figure 4

Conceptual framework of the study area.

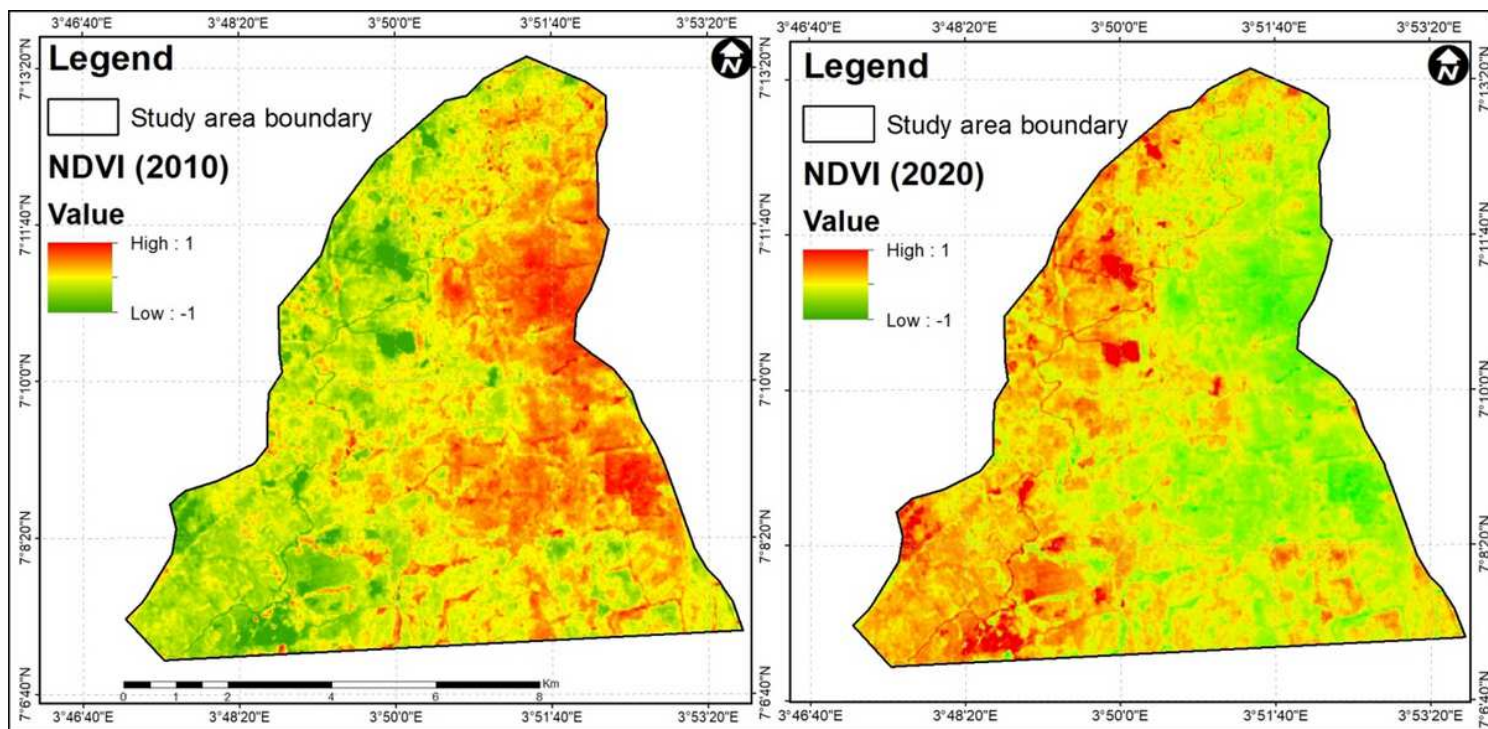


Figure 5

Normalized difference vegetation index of the study area

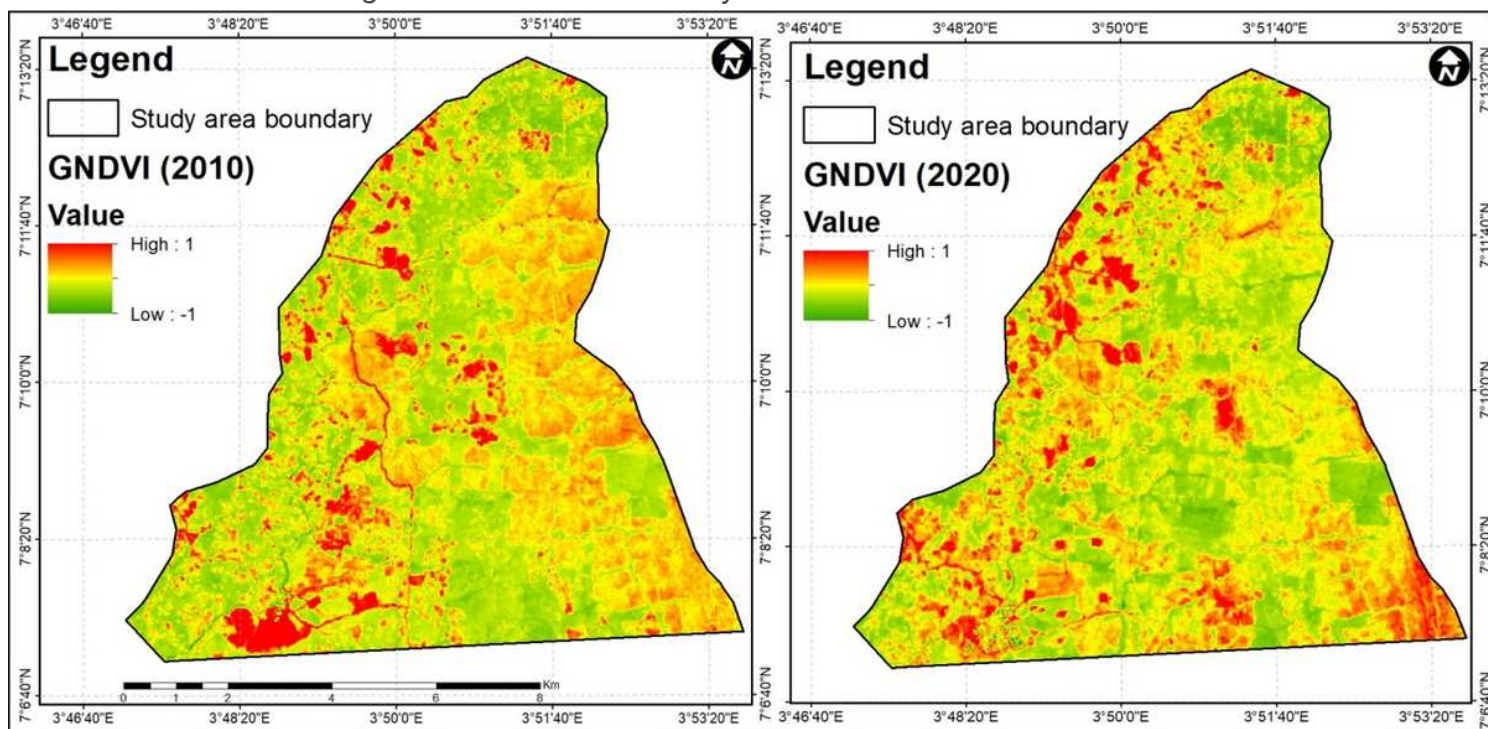


Figure 6

Green Normalized vegetation index of the study area

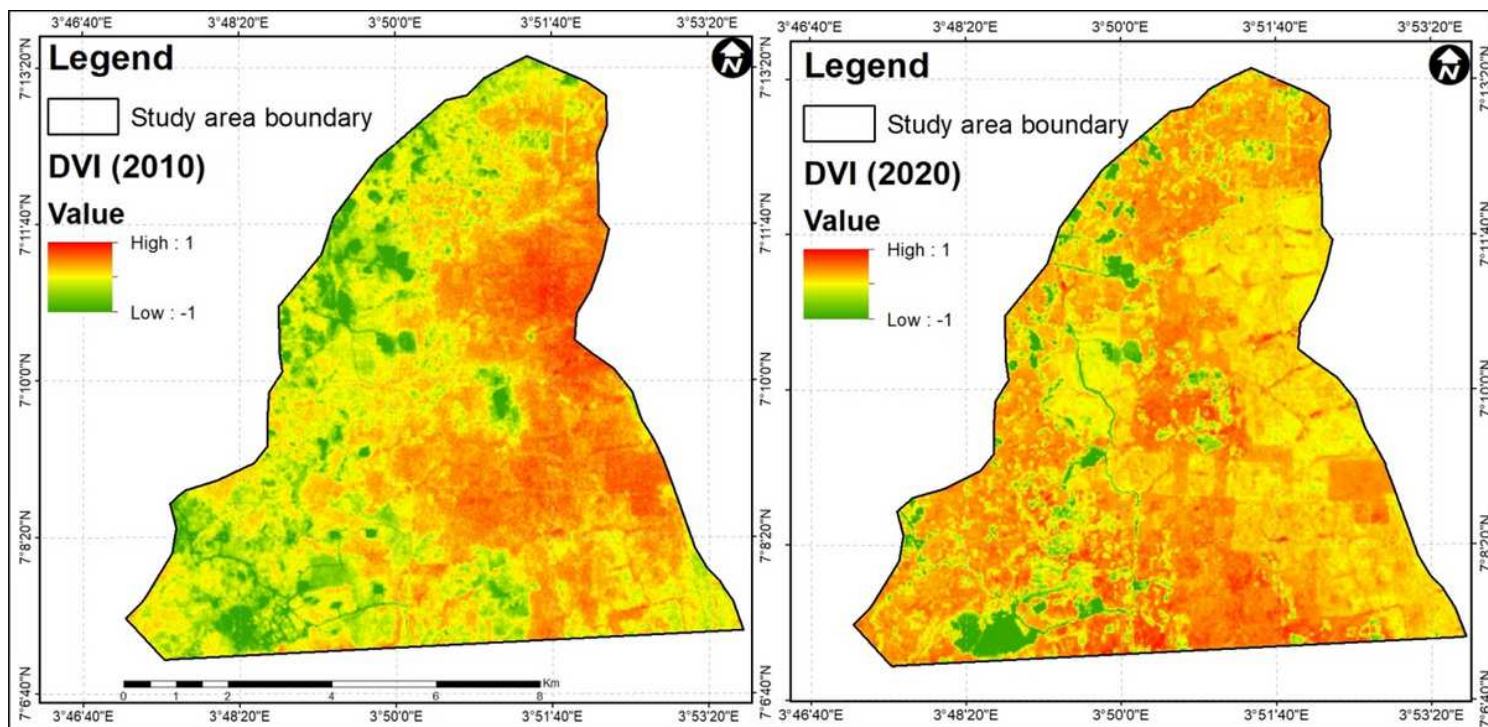


Figure 7

Difference vegetation index of the study area

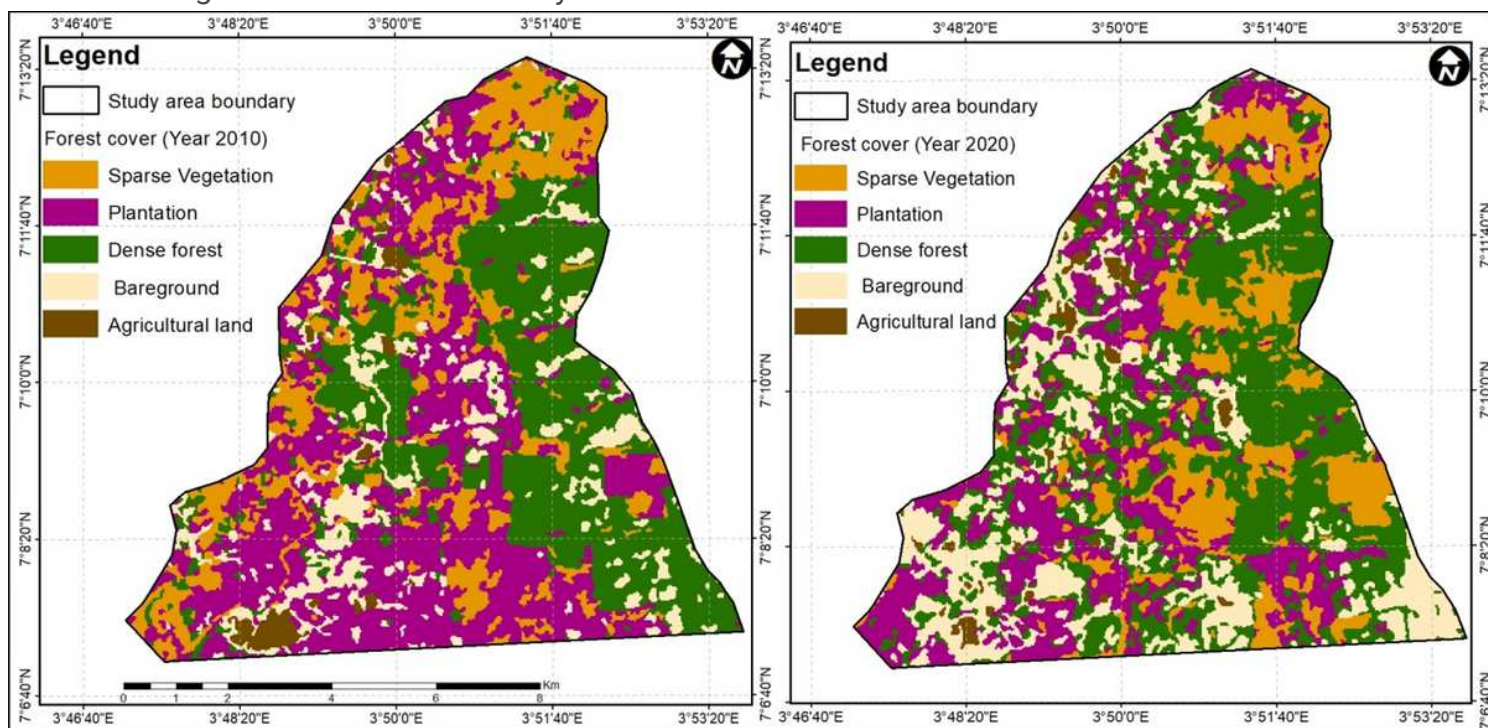


Figure 8

Forest cover map for the year 2010 and 2020

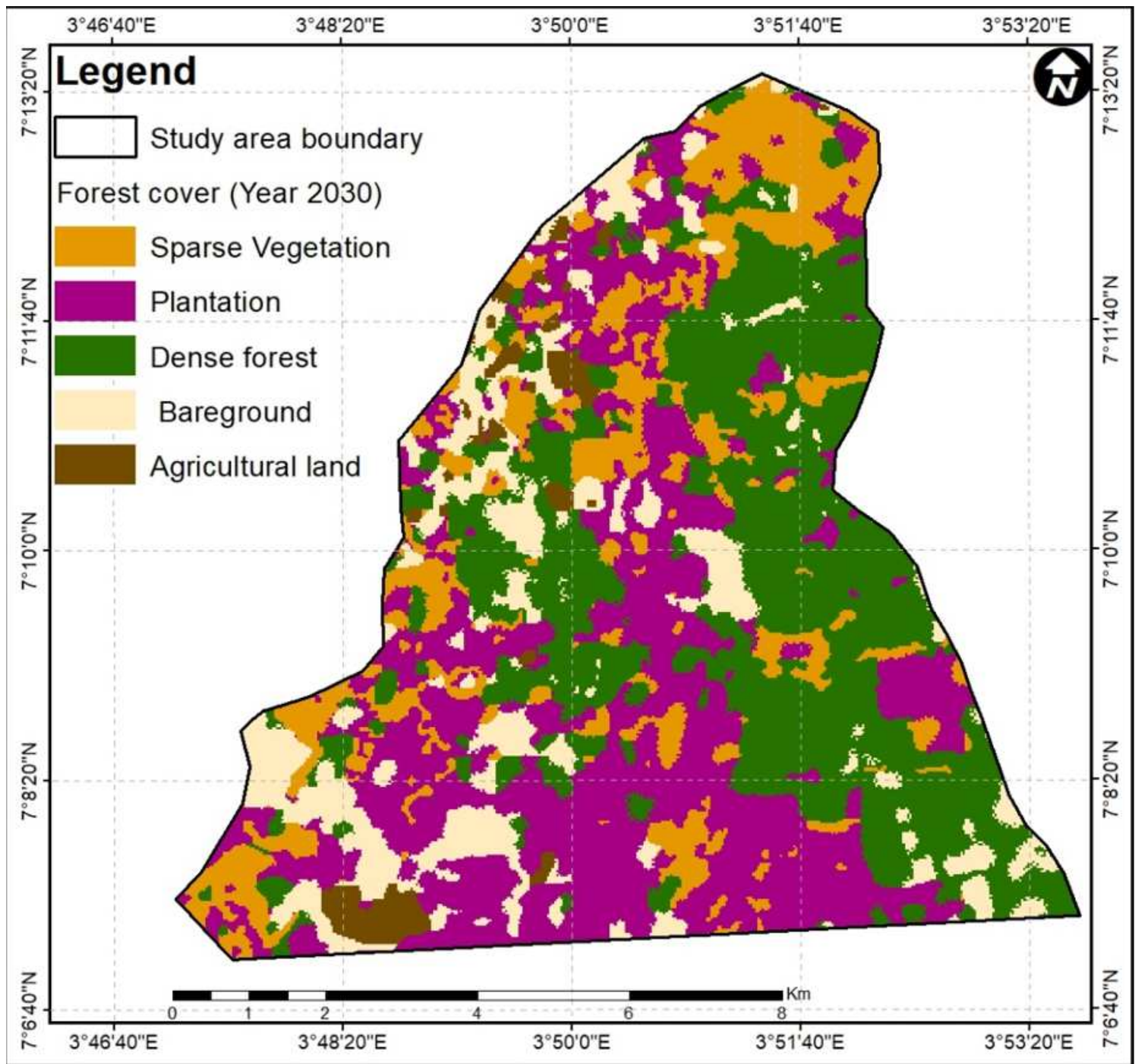


Figure 9

Forest cover map for the year 2030